



Adsorption behavior of Crystal Violet dye in aqueous solution using Co^{+2} hectorite composite as adsorbent surface

Ahmed Jaber Ibrahim^{a,*}

^a Scientific Research Center, Al-Ayen University, ThiQar 64011, Iraq

ARTICLE INFO:

Received 15 Nov 2022

Revised form 1 Feb 2023

Accepted 25 Feb 2023

Available online 30 Mar 2023

Keywords:

Adsorption,
UV-Vis spectrophotometer,
Crystal violet,
Isotherm,
Thermodynamics,
Kinetics

ABSTRACT

This study focused on the adsorption behavior of the cationic Crystal Violet (CV) dye from aqueous solutions using a Co^{+2} -hectorite composite as an adsorbent surface. The initial and equilibrium CV dye concentrations were determined using a UV-Vis spectrophotometer. The results were discussed and presented for the impacts of pH, primary CV dye concentration, composite dosage, and temperature. The optimum conditions were found for eliminating Crystal Violet dye from the aqueous solution at a pH 4, ideal temperature 293 K, and 0.5 g L^{-1} of composite dose. The pseudo-second-order kinetic, intraparticle diffusion analyzed the tests' data and film diffusion models. Each model's defining features have been identified, and these models were in good agreement and in charge of regulating the adsorption reaction. The adsorption operation was also thermodynamically examined to determine thermodynamic variables such as Gibbs free energy (ΔG°), entropy (ΔS°), activation energy (E_a), and enthalpy (ΔH°). The negative value of Gibbs free energy (ΔG°) and enthalpy (ΔH°) indicated that the adsorption process was a spontaneous and exothermic reaction. While the activation energy (E_a) data which fell within the normal range for physisorption, was discovered to be $22.434 \text{ kJ mol}^{-1}$. This result proved that physical adsorption occurs between the CV dye and the adsorbent surface (Co^{+2} -hectorite composite).

1. Introduction

Although synthetic dyes are widely utilized in the textile sector, 20 to 40 % of these pigments still end up in effluents [1-3]. The majority of pigments contain hazardous and cancer-causing substances. They also pose a significant hazard to the health of people and the environment since they are resistive and so stable in a recovering ecosystem [4]. Therefore, before the dye-containing wastewater is released into the environment, the dyes must be removed to safeguard persons and ecosystems

from pollution. The elimination of contaminants in plastics, pulp, dyestuffs, paper effluents, and textiles has been documented using several physical, chemical, and biological decolorization processes. However, these sectors had only welcomed a small number of them [5–18]. Adsorption is the best option for producing the most significant outcomes among the several dye removal procedures since it may be used to eliminate specific groups of chemical contaminants from aqueous solutions. Adsorption is preferable to compete for systems for utilizing recycled water regarding low cost, formability and styling simplicity, ease of use, and sensitivity to harmful contaminants. According to several studies

*Corresponding Author: Ahmed Jaber Ibrahim

Email: ahmed.jibrahim@alayen.edu.iq

<https://doi.org/10.24200/amecj.v6.i01.219>

[19,20], activated charcoal and polymer resins are the best adsorbents for eliminating pigments from suitably saturated sewage. The adsorption capability of some reactive dyes by activated carbon is known to be relatively poor. The sewage treatment process utilizing clay-basic [21], AC-ZnO nanostructure [22], cotton [23], Ultraviolet-activated sodium perborate [24], halloysite nanotubes [25], electrospun nanofiber mat [26], chitosan [27], and natural zeolite-basic [18] has thus been the subject of Previous studies. Because of their large surface area and molecular sieve composition, Clay-based materials are efficient organic cation pollutant adsorbents [3]. The generality widely utilized layered silicate is hectorite. Tetrahedral substituted and octahedral substituted are the two structural kinds. Hectorite is an excellent adsorbent for eliminating dye from comparatively saturated wastewater. This is attributed to the fact that hectorite has a unique structure with internal channels that permits the passage of solutes and bonded organic and inorganic ions into the structure of hectorite. This article suggested using a Co^{+2} -hectorite composite as an Adsorbent surface to absorb crystal violet (CV) dye from aqueous solutions. The results were discussed and presented for the impacts of pH, primary CV dye concentration, composite dosage, and temperature. The data from the tests were analyzed by the pseudo-second-order kinetic, intra-particle diffusion, and film diffusion models. Each model's defining features have been identified. The adsorption operation was also thermodynamically examined to determine thermodynamic variables such as Gibbs free energy (ΔG°), entropy (ΔS°), activation energy (E_a), and enthalpy (ΔH°).

2. Materials and Methods

2.1. Instruments

Thermostatic Controlled shaker (SHKE4000, Thermo Fisher Scientific; USA), UV-Vis spectrophotometer (UV-3600i Plus, Shimadzu, Japan), pH meter (model 744 Metrohm; Germany), Ultrasonic cleaner (WUC-A 1,2- Witeg Labortechnik GmbH; Germany), Mechanical stirrer (Eurostar 60 digital, IKA; China) and vacuum drying oven (Model VD 56-BINDER GmbH; Germany) were used.

2.2. Chemicals

All chemicals with high purity were purchased from the original Company. The chemicals such as, Crystal Violet (CV) dye ($\text{C}_{25}\text{H}_{30}\text{ClN}_3$, Mwt 407.986 dalton, CAS N.: 548-62-9, Tokyo Chemical Industry Co., Japan; Fig. 1), hectorite ($\text{Na}_{0.3}(\text{Mg}, \text{Li})_3\text{Si}_4\text{O}_{10}(\text{OH})_2$, Mwt 360.58 dalton, CAS N.: 12173-47-6, Spectrum Chemical Co., USA), hydrochloric acid 37% (HCL, CAS N.: 7647-01-0, Sigma-Aldrich Chemie GmbH Co., USA), and Cobalt chloride (CoCl_2 , CAS N.: 7646-79-9, American Elements Co., USA) were prepared for this research.

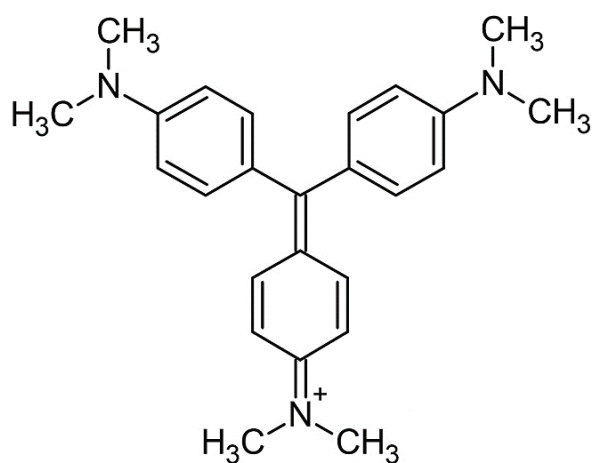


Fig. 1. The structural formula of Crystal Violet dye

2.3. Preparation of Co^{+2} -hectorite composite

The ion-exchanged technique was used to prepare the sorbent in a single step. Two grams of hectorite were mixed with 0.2 liters of distilled water and swirled for 2 hours. Using hydrochloric acid (1M, HCl) solution, the colloidal dispersion's pH was reduced to 6. Cobalt chloride (CoCl_2) solution was added in the calculated amount while stirring for 8 hours. The final dispersion was cleaned by distilled water. At 80°C , the product was dried after centrifugation.

2.4. Adsorbate

Crystal Violet (CV) dye was used as the model guest to examine the adsorption capability. Using a UV-Vis spectrophotometer with a range of 200 - 800 nm, the

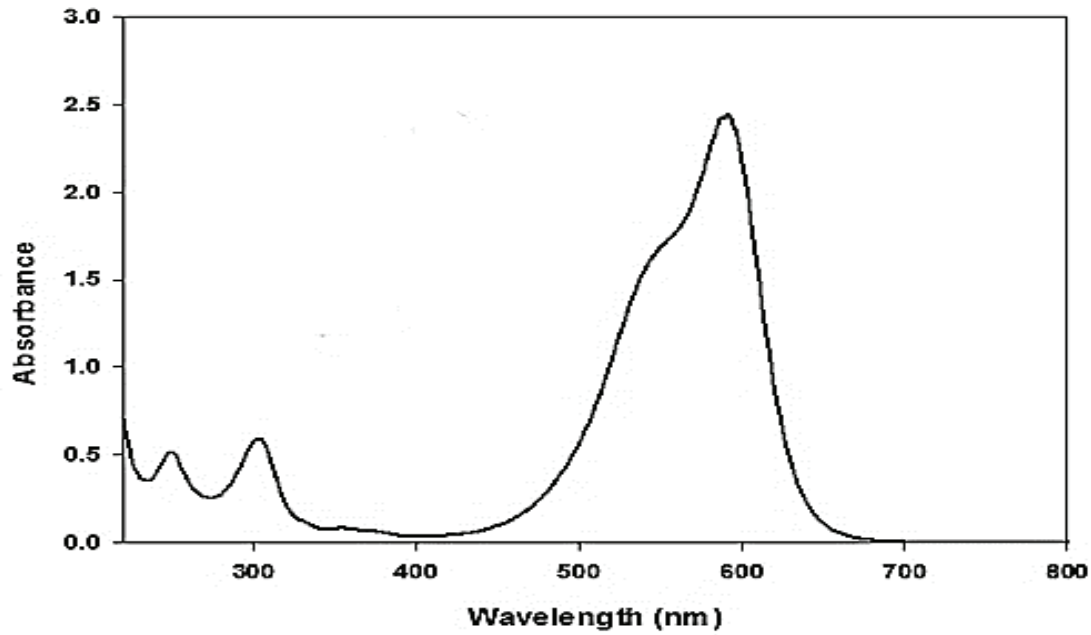


Fig. 2. The UV-Vis spectrum of Crystal violet dye

maximum wavelength of 585 nm was determined, which corresponds to the highest absorption of the dye solution, as shown in Figure 2. To create the stock solution, distilled water was used to dissolve a carefully weighed quantity of CV dye. The solutions for adsorption testing were made at the necessary concentrations by applying serial dilutions to the stock solution. First, a calibration curve for CV dye was drawn. In kinetic and thermodynamic studies, this curve was used to translate data on concentration from absorbance measurements.

2.5. Adsorption process

At various temperatures, adsorption studies were conducted in a controlled thermostatic shaker. Up until the point of equilibrium, the shaking persisted. The initial and equilibrium CV dye concentrations were determined using a UV-Vis spectrophotometer. The adsorption capability of the adsorbent was determined using these data. It was possible to determine the quantity of CV adsorbed (q_e) at equilibrium. The mass balance is shown in Equation 1.

$$q_e = v(C_0 - C_e) / W \quad (\text{Eq.1})$$

Where v is the volume of dye solution used (L), C_0 is the primary dye concentration in the liquid phase (g L^{-1}), C_e is the liquid phase dye concentration at equilibrium (g L^{-1}), and W is the mass of sorbent utilized (g). By adding 0.03 g sorbent at various temperatures to 0.060 L of crystal violet solution (0.150 g L^{-1}), kinetic investigations were conducted. The liquid phase crystal violet concentration was monitored at predetermined intervals.

3. Results and Discussion

3.1. The influence of solution pH

The influence of solution pH for the elimination of CV dye by Co^{+2} -hectorite complex was studied in the range of 2–12 under the conditions: 0.150 g L^{-1} CV dye concentration, 0.5 g L^{-1} Composite dosages, 293 temperature, and 1 hour Contact time). The implies of the repeated experimental outcomes are plotted in Figure 3. The experimental results showed that the degree of adsorption of CV dye on the Co^{+2} -hectorite composite reached 95% when the pH of the solution was 4. Therefore, the optimal pH was considered to be 4, which achieves the maximum adsorption of CV dye. On this basis, the remainder of the subsequent tests were carried out at this optimum pH value. Other investigators

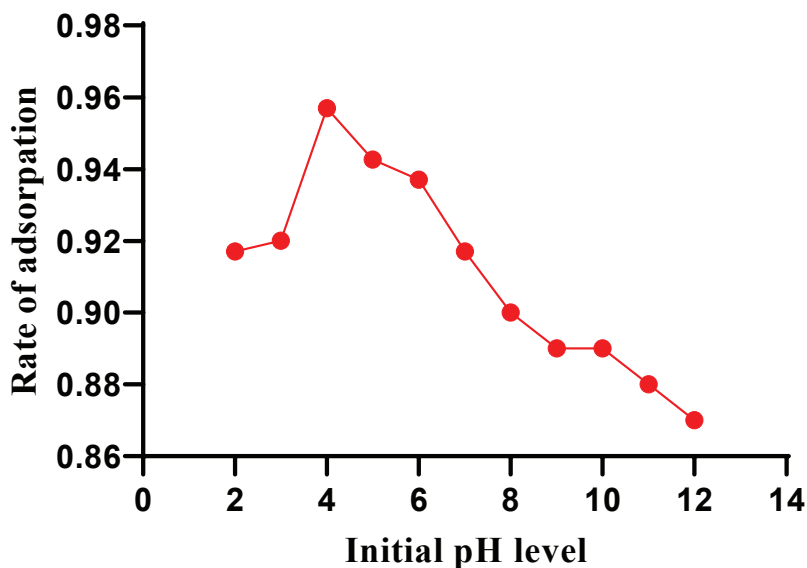


Fig. 3. Influence of pH of CV dye adsorption on Co^{+2} -hectorite composite

have shown a tendency similar to the adsorption process of the Congo red azo dye as a function of pH [28].

3.2. Effect of sorbent composite dose

Between 0.5 and 1.5 g L^{-1} of Co^{+2} -hectorite composite, the dose was tested under the conditions: (primary CV dye concentration 0.5 g L^{-1} , 0.6 g L^{-1} , 0.7 g L^{-1} , $\text{pH}=4$, 293 K temperature and 8 hour Contact time) to see how it affected CV dye adsorption. Figure 4 of the findings indicates a decrease in q_e with an increase in Co^{+2} -hectorite dosage. Because a greater adsorbent dose decreases the adsorption sites' unsaturation, there is relatively

less adsorption at larger adsorbent doses. CV dye can quickly arrive at the adsorption locations, and the q_e rises when the amount of adsorbent is modest. Because less of the adsorbent's adsorptive capacity is being utilized with an increase in adsorbent amount, the correlating increase in adsorption reaction per unit cluster is decreased.

Higher adsorbent dosages caused particle aggregation, reducing the overall surface area and the multitude of active adsorption locations. The highest CV dye adsorption in this research was accomplished at a Co^{+2} -hectorite dose of 0.5 g remaining trials were carried out at this concentration.

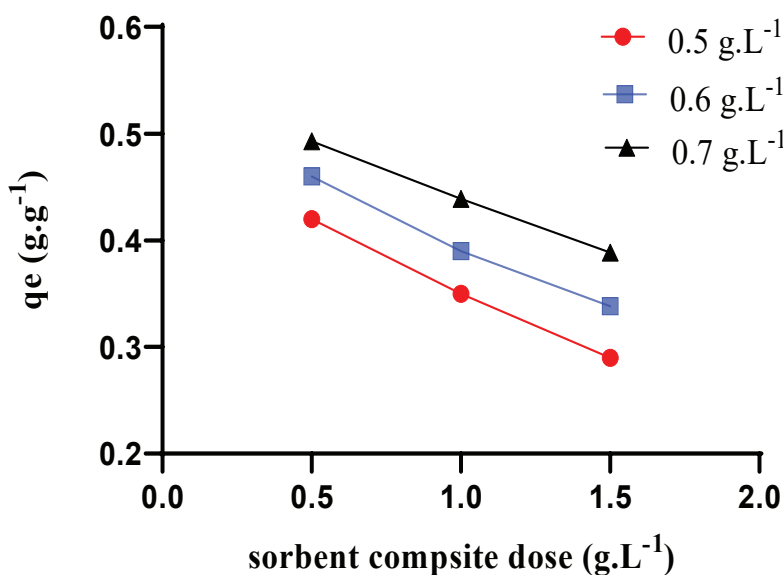


Fig. 4. Effect of sorbent composite dose on CV dye adsorption

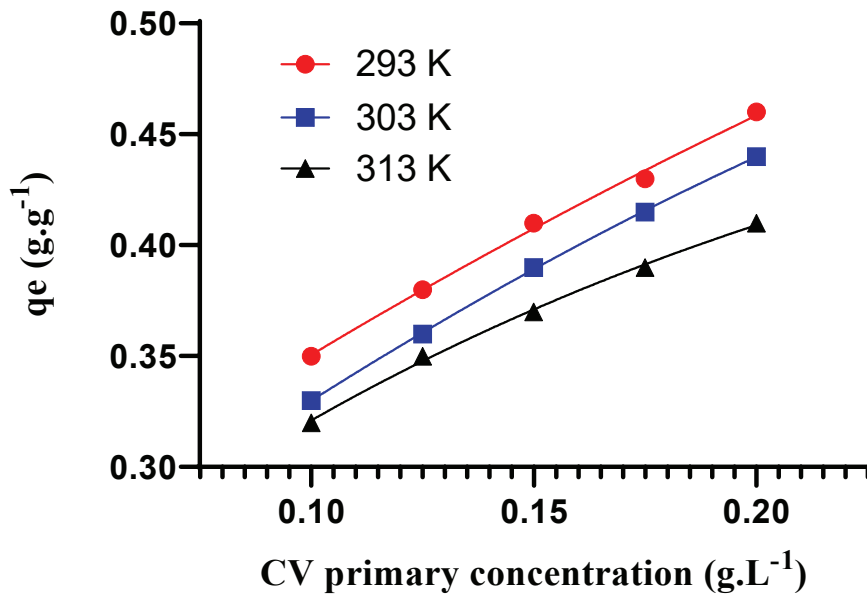


Fig. 5. Influence of primary dye concentration and temperature on the adsorption process

3.3. Effect of primary crystal violet (CV) dye concentration and temperature

It is unclear how varied CV dye concentrations affect how well Co²⁺-hectorite composite removes CV because the effluent from various industries may include varying amounts of dye. This study examined the adsorption of concentrations of 0.100, 0.125, 0.150, 0.175, and 0.200 g L⁻¹ CV dye for the Co²⁺-hectorite composite. The duplicate data's means are shown in Figure 5, which shows that the concentration of CV dye has a significant influence on the adsorption capability of the Co²⁺-hectorite composite. Based on the data shown in Figure 5, the q_e of Co²⁺-hectorite rose at various temperatures when the primary CV dye concentration was raised. This is explained by the reality that free adsorption locations are accessible at the start of the test and by the fact that there was a more effective mass transfer rate during the first contact period when the CV dye concentration was at its highest.

The impact of temperature on the CV dye adsorption equilibrium on the Co²⁺-hectorite surface is also depicted in Figure 5. For a primary concentration of 0.100-0.200 g L⁻¹, it can be seen that the q_e declined as the temperature rose, indicating an exothermic process. Though the impact of temperature on the

adsorption equilibrium was negligible at the low starting concentration of CV dye (0.100 g L⁻¹), it was still present.

3.4. The investigation of intra-particle diffusion and film diffusion

To determine whether external film diffusion or intraparticle diffusion affected the removal rate, the Weber-Morris kinetic model was used as Equation 2[29].

$$qt = K_{id}t^{0.5} + C \quad (\text{Eq.2})$$

where q_t represents the removal capacity (mg g⁻¹) at time(t), K_{id} represents the intra-particle diffusion rate constant (mg per g min^{0.5}), and C represents a constant whose value is proportionate to the limit layer (mg g⁻¹).

When the adsorption system corresponds with the intra-particle diffusion mechanism, a plot of q_t versus $t^{0.5}$ should have a straight line with a slope of K_{id} and an intercept of C, according to Equation 2. Figure 6 shows a plot of the means of the replicated experimental outcomes. There are two distinct zones in Figure 6. The first straight and the second linear sections are attributed to macro- and micro-

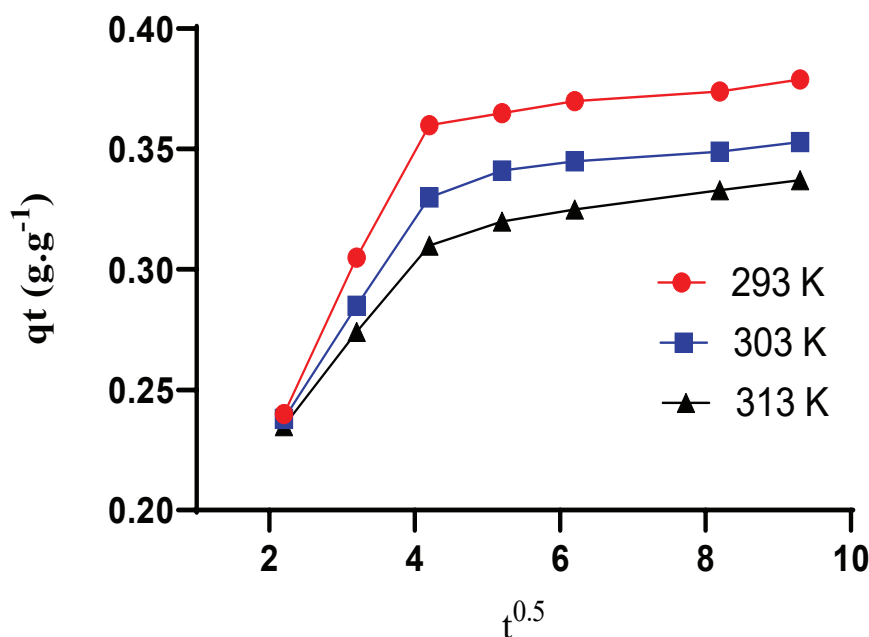


Fig. 6. Scatter plot of qt versus $t^{0.5}$ for adsorption of CV dye on Co^{+2} -hectorite composite at studied temperatures

pore diffusion, respectively. The immediate use of the adsorbing locations on the adsorbent superficial is blamed in the first section. The second section's phenomenon is linked to an extremely slow CV diffusion into the least accessible adsorption sites—the micro-pores—from the surface film. Additionally, this promotes the sluggish quiet rate of adsorbate movement from the liquid stage to the surface of the adsorbent. The mass transfer rate variance between the adsorption reaction's first and end phases explains why the straight line deviates from the original line. The straight line's continued departure from the point of origin suggests that pore diffusion is not the lone rate-limiting process [30].

To support the above findings, the intra-particle diffusion coefficients (D_p) were estimated by Equation 3.

$$D_p = \frac{(0.03 r_0^2)}{t^{0.5}} \quad (\text{Eq.3})$$

where r_0 (m) represents the mean radius of the adsorbent particles and $t^{0.5}$ (min) the time needed to fulfill half of the adsorption.

The rate-limiting phase will be intra-particle diffusion, referring to Sushanta et al. [31], if the predicted intra-particle diffusion coefficient (DP) level is in the scope 10^{-15} - 10^{-18} m^2 per S. According to Table 1, which was used in this investigation, the computed DP level varied from 1.65×10^{-14} to 2.47×10^{-14} $\text{m}^2 \text{ s}^{-1}$ at various temperatures, implying that intra-particle diffusion reaction is not the primary process limiting CV dye adsorption onto Co^{+2} -hectorite surface.

Table 1. The adsorption process's film diffusion coefficient (DF) and intra-particle diffusion coefficients (DP) at the temperatures studied

Temperature (k)		DP ($\text{m}^2 \text{ S}^{-1}$)	DF ($\text{m}^2 \text{ S}^{-1}$)	r_0 (m)
293	77.44	1.65×10^{-14}	3.44×10^{-13}	6.54×10^{-4}
303	63.36	2.02×10^{-14}	4.21×10^{-13}	
313	51.87	2.47×10^{-14}	5.63×10^{-13}	

Equation 4 has been used to compute the film diffusion coefficients (DF), to examine the adsorption kinetics reactions.

$$DF = \frac{(0.23 r_0 \delta C_s)}{(Cl t_{0.5})} \quad (\text{Eq.4})$$

Where C_s is the concentration of adsorbate in the solid phases, C_l is the concentration of adsorbate in the liquid phase, and r_0 and $t_{0.5}$ share the identical meaning as earlier, and d is the film thickness (10^{-5}m) [31]. The computed film diffusion coefficient (DF) value will fall between 10^{-10} and $10^{-12} \text{ m}^2 \text{ per second}$ if the film diffusion reaction is the rate-limiting step's controlling factor. The predicted levels of DF were discovered to be in the arrange of $10^{-13} \text{ m}^2 \text{ s}^{-1}$ (Table 1), indicating that the film diffusion reaction was not the lone phase in the adsorption process that was rate-limiting. Intra-particle and film diffusions in this study served to regulate the kinetic process. The kinetic reaction was governed by film diffusion since the CV concentration was high at the beginning of the adsorption process. CV molecules started to diffuse inside Co^{+2} -hectorite when they were adsorbed on the surface of the composite, and the adsorption reaction was what controlled this.

3.5. Thermodynamics study

The pseudo-second-order [32] model has been investigated about kinetic modeling to determine the adsorption mechanism (Equation 5).

$$\frac{t}{qt} = \frac{1}{k_2 q_e^2} + \frac{1}{q_e} t \quad (\text{Eq.5})$$

Where q_e is the equilibrium adsorption capability (g.g^{-1}), k_2 is the pseudo-second-order adsorption rate constant (g min g^{-1}), and qt is the amount of CV adsorbed at time t (g g^{-1}). To determine rate parameters, the straight line plots of t/qt vs. t for the pseudo-second-order models have also been investigated (Fig. 7). Table 2 contains the correlation coefficients r^2 , k , and q_e at numerous temperatures. The Arrhenius equation (Eq. 6) can express the pseudo-second-order rate constants as a temperature performance.

$$\ln k = \ln A - Ea/RT \quad (\text{Eq.6})$$

Where k is the rate constant, A is the frequency coefficient, E_a is the activation energy, R is the gas constant, and T is the temperature in Kelvin.

Figure 8 shows a visualization of the means of the replicated experimental outcomes.

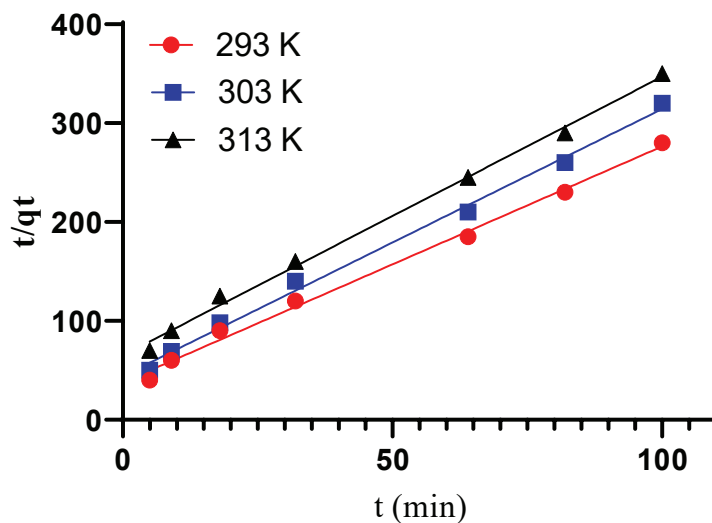


Fig. 7. The pseudo-second-order kinetics model for the adsorption of CV dye onto Co^{+2} -hectorite composite at studied temperatures

Table 2. The Arrhenius activation energy (E_a) and pseudo-second-order kinetics parameter values for the adsorption process at temperatures studied

Temperature (k)	(kJ mol ⁻¹)	r ²	qe (g g ⁻¹)	k ²
293	22.434	0.9996	0.335	2.087
303		0.9954	0.317	2.794
313		0.9965	0.302	3.587

The E_a is calculated using Equation 6 (Table 2). The size of the activation energy gives a clue as to the primary kind of adsorption, either chemical or physical. Physisorption processes typically have activation energies between 5 and 40 kJ mol⁻¹, whereas greater activation energies (between 40 and 800 kJ.mol⁻¹) point to chemisorption. The dispersive interaction between the crystal violet and the Co⁺²-hectorite surface implies it. The Gibbs free energy (ΔG°), enthalpy change (ΔH°), and entropy change (ΔS°), which are thermodynamic characteristics, have been calculated to assess the viability and exothermic characteristic of the

adsorption reaction. Equation 7 relates the process's change in Gibbs free energy to the equilibrium constant (k).

$$\Delta G_0 = -RT \ln K \quad (\text{Eq. 7})$$

The below formula shows how the standard free energy change at constant temperature is also correlated with enthalpy and entropy changes (Eq. 8).

$$\ln K = -\frac{\Delta H_0}{RT} + \frac{\Delta S_0}{R} \quad (\text{Eq. 8})$$

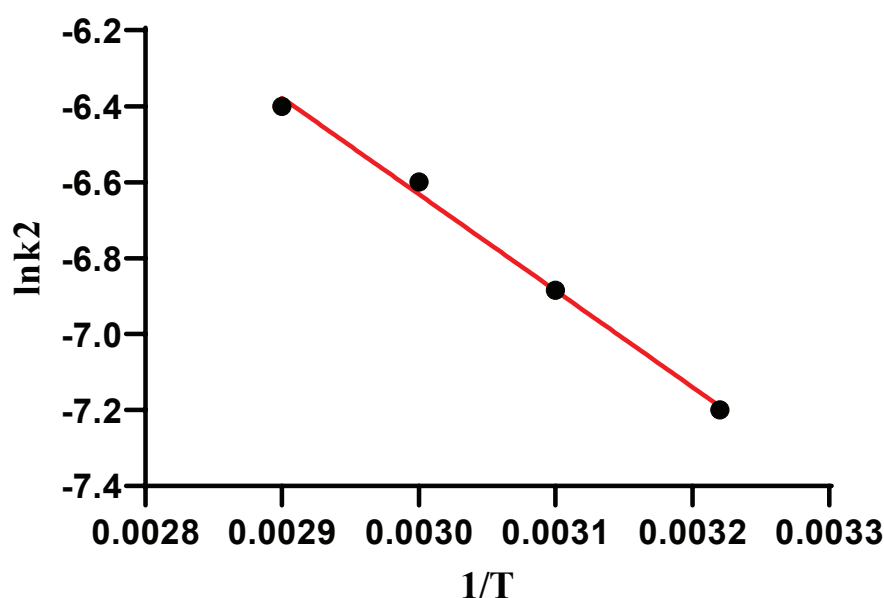


Fig. 8. Arrhenius Scatter plots for the adsorption of CV dye onto Co⁺²-hectorite at studied temperatures

The slope and intercept of Scatter plots of $\ln k$ vs $1/T$ are utilized to evaluate the levels of ΔG° and ΔS° (Fig. 9). Table 3 contains the obtained values. Indicating the viability and spontaneity of the CV adsorption reaction on the Co^{+2} -hectorite surface, the Gibbs free energy (ΔG°) levels were observed to be decreasingly negative with temperature. It is discovered that the enthalpy change (ΔH°) values are negative, indicating the exothermic character of the adsorption process. The fact that the (ΔH°) value is less than $40 \text{ kJ}\cdot\text{mol}^{-1}$ shows that the crystal violet adsorption by the composite of Co^{+2} -hectorite is physisorption. The results from the current study are comparable to those from Xia's study [28] on the adsorption reaction of congo red azo dye from aqueous solution by ODA-hectorite and CTAB-hectorite as adsorbent surfaces.

4. Conclusion

The results of this investigation demonstrate the efficiency of Co^{+2} -hectorite composite as an adsorbent surface for eliminating Crystal Violet (CV) dye from aqueous solutions. The elimination of CV worked best at a pH of 4. The ideal temperature and composite dose were 293°K and 0.5 g L^{-1} , respectively. The experimental results and the pseudo-second-order kinetic model were in good agreement, as indicated by the straight lines in t/qt vs t plots. Intra-particle and film diffusions were in charge of regulating the adsorption reaction. The exothermic and spontaneous response of CV adsorption on Co^{+2} -hectorite composite is revealed by evaluating the thermodynamic parameters. The activation energy for adsorption, which fell within the normal range for physisorption, was discovered

Table 3. Thermodynamic variables for the adsorption process

Temperature (k)	Distribution coefficient (k)	ΔG° (kJ mol ⁻¹)	ΔH° (kJ mol ⁻¹)	ΔS° (kJ mol ⁻¹)
293	4.654	-3.745		
303	3.324	-2.926	-31.546	-94.883
313	2.067	-1.768		

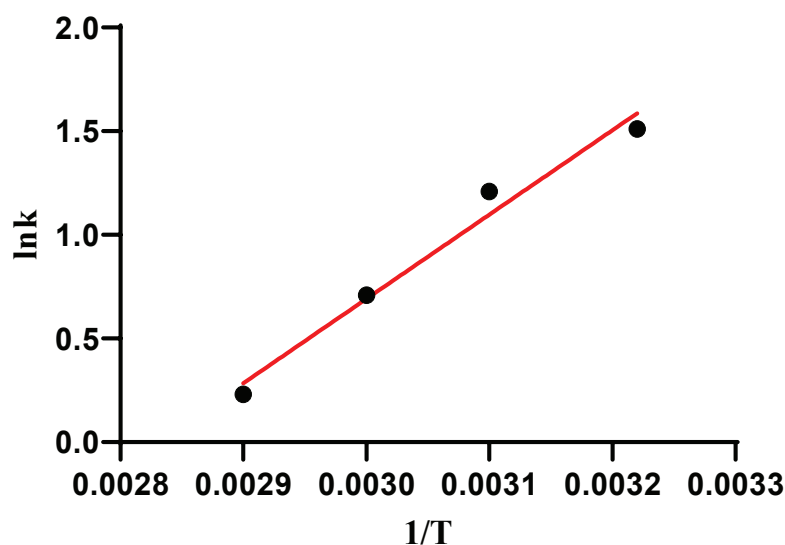


Fig. 9. Scatter plot of $\ln k$ vs. $1/T$ for CV dye adsorption onto Co^{+2} -hectorite composite.

to be 22.434 kJ mol⁻¹. The outcomes would benefit the design of wastewater treatment facilities that remove the dye.

5. Acknowledgements

The structural formula of the Physical Chemistry Lab., Chemistry Department, College of Education for Pure Science (Ibn-al Haitham), University of Baghdad, supports this research.

6. References

- [1] F. Kooli, S. Rakass, Y. Liu, M. Abboudi, H.O. Hassani, S.M. Ibrahim, F. Wadaani, R. Al-Faze, Eosin removal by Cetyl trimethylammonium-Cloisites: influence of the surfactant solution type and regeneration properties, *Mol.*, 24 (2019) 3015. <https://doi.org/10.3390/molecules24163015>.
- [2] F.M. Valadi, A. Ekramipooya, M.R. Gholami, Selective separation of Congo Red from a mixture of anionic and cationic dyes using magnetic-MOF: Experimental and DFT study, *J. Mol. Liq.*, 318 (2020) 114051. <https://doi.org/10.1016/j.molliq.2020.114051>.
- [3] P. S. Kumar, G. J. Joshiba, C. C. Femina, P. Varshini, S. Priyadarshini, M. A. Karthick, R. Jothirani, A critical review on recent developments in the low-cost adsorption of dyes from wastewater, *Desalin. Water Treat.*, 172 (2019) 395-416. <https://doi.org/10.5004/dwt.2019.24613>.
- [4] S. Benkhaya, S. M'rabet, A. El Harfi, Classifications, properties, recent synthesis and applications of azo dyes, *Heliyon*, 6 (2020) e03271. <https://doi.org/10.1016/j.heliyon.2020.e03271>.
- [5] G. Crini, E. Lichtfouse, Advantages and disadvantages of techniques used for wastewater treatment, *Environ. Chem. Lett.*, 17 (2019) 145-155. <https://doi.org/10.1007/s10311-018-0785-9>.
- [6] S. Samsami, M. Mohamadizani, M.H. Sarrafzadeh, E.R. Rene, M. Firoozbahr, Recent advances in the treatment of dye-containing wastewater from textile industries: Overview and perspectives, *Proc. Safe. Environ. Prot.*, 143 (2020) 138-163. <https://doi.org/10.1016/j.psep.2020.05.034>.
- [7] E. Routoula, S.V. Patwardhan, Degradation of anthraquinone dyes from effluents: a review focusing on enzymatic dye degradation with industrial potential, *Environ. Sci. Technol.*, 54 (2020) 647-664. <https://doi.org/10.1021/acs.est.9b03737>.
- [8] A. Tkaczyk, K. Mitrowska, A. Posyniak, Synthetic organic dyes as contaminants of the aquatic environment and their implications for ecosystems: A review, *Sci. Total Environ.*, 717 (2020) 137222. <https://doi.org/10.1016/j.scitotenv.2020.137222>.
- [9] L. Largette, R. Pasquier, A review of the kinetics adsorption models and their application to the adsorption of lead by an activated carbon, *Chem. Eng. Res. Des.*, 109 (2016) 495-504. <https://doi.org/10.1016/j.cherd.2016.02.006>.
- [10] C. Santhosh, V. Velmurugan, G. Jacob, S.K. Jeong, A.N. Grace, A. Bhatnagar, Role of nanomaterials in water treatment applications: a review, *Chem. Eng. J.*, 306 (2016) 1116-1137. <https://doi.org/10.1016/j.cej.2016.08.053>.
- [11] M. Berradi, R. Hsissou, M. Khudhair, M. Assouag, O. Cherkaoui, A. El Bachiri, A. El Harfi, Textile finishing dyes and their impact on aquatic environs, *Heliyon*, 5 (2019) e02711. <https://doi.org/10.1016/j.heliyon.2019.e02711>.
- [12] M.T. Yagub, T.K. Sen, S. Afroze, H.M. Ang, Dye and its removal from aqueous solution by adsorption: a review, *Adv. Coll. Inter. Sci.*, 209 (2014) 172-184. <https://doi.org/10.1016/j.cis.2014.04.002>.
- [13] T.A. Saleh, Protocols for synthesis of nanomaterials, polymers, and green materials as adsorbents for water treatment technologies, *Environ. Tech. Innov.*, 24

- (2021) 101821. <https://doi.org/10.1016/j.eti.2021.101821>.
- [14] X. Liu, H. Pang, X. Liu, Q. Li, N. Zhang, L. Mao, M. Qiu, B. Hu, H. Yang, X. Wang, Orderly porous covalent organic frameworks-based materials: superior adsorbents for pollutants removal from aqueous solutions, *Innovation*, 2 (2021) 100076. <https://doi.org/10.1016/j.xinn.2021.100076>.
- [15] I.C. Ossai, A. Ahmed, A. Hassan, F.S. Hamid, Remediation of soil and water contaminated with petroleum hydrocarbon: A review, *Environ. Tech. Innov.*, 17 (2020) 100526. <https://doi.org/10.1016/j.eti.2019.100526>.
- [16] J. Liu, G. Zhang, Recent advances in synthesis and applications of clay-based photocatalysts: a review, *Phys. Chem. Chem. Phys.*, 16 (2014) 8178-8192. <https://doi.org/10.1039/C3CP54146K>.
- [17] Z. Wang, Z. Wang, S. Lin, H. Jin, S. Gao, Y. Zhu, J. Jin, Nanoparticle-templated nanofiltration membranes for ultrahigh performance desalination, *Nat. comm.*, 9 (2018) 1-9. <https://doi.org/10.1038/s41467-018-04467-3>.
- [18] D. Yue, Y. Jing, J. Ma, C. Xia, X. Yin, Y. Jia, Removal of neutral red from aqueous solution by using modified hectorite, *Desalination*, 267 (2011) 9-15. <https://doi.org/10.1016/j.desal.2010.08.038>
- [19] N.U.M. Nizam, M.M. Hanafiah, E. Mahmoudi, A.A. Halim, A.W. Mohammad, The removal of anionic and cationic dyes from an aqueous solution using biomass-based activated carbon, *Sci. Rep.*, 11 (2021) 1-17. <https://doi.org/10.1038/s41598-021-88084-z>
- [20] C.F. Mok, Y.C. Ching, F. Muhamad, N.A. Abu Osman, N.D.Hai, C.R. Che Hassan, Adsorption of dyes using poly (vinyl alcohol)(PVA) and PVA-based polymer composite adsorbents: a review, *J. Poly. Environ.*, 28 (2020) 775-793. <https://doi.org/10.1007/s10924-020-01656-4>
- [21] I. Chaari, E. Fakhfakh, M. Medhioub, F. Jamoussi, Comparative study on adsorption of cationic and anionic dyes by smectite rich natural clays, *J. Mol. Struct.*, 1179 (2019) 672-677. <https://doi.org/10.1016/j.molstruc.2018.11.039>
- [22] A.J. Ibrahim, ZnO nanostructure synthesis for the photocatalytic degradation of azo dye methyl orange from aqueous solutions utilizing activated carbon, *Anal. Meth. Environ. Chem. J.*, 5 (2022) 5-19. <https://doi.org/10.24200/amecj.v5.i04.200>
- [23] A.N.M.A. Haque, R. Remadevi, O.J. Rojas, X. Wang, M. Naebe, Kinetics and equilibrium adsorption of methylene blue onto cotton gin trash bioadsorbents, *Cellulose*, 27 (2020) 6485-6504. <https://doi.org/10.1007/s10570-020-03238-y>
- [24] A.J. Ibrahim, Ultraviolet-activated sodium perborate process (UV/SPB) for removing humic acid from water, *Anal. Meth. Environ. Chem. J.*, 5 (2022) 5-18. <https://doi.org/10.24200/amecj.v5.i03.191>
- [25] Y.M. Vargas-Rodríguez, A. Obaya, J.E. García-Petronilo, G.I. Vargas-Rodríguez, A. Gómez-Cortés, G. Tavizón, J.A. Chávez-Carvayar, Adsorption studies of aqueous solutions of methyl green for halloysite nanotubes: Kinetics, isotherms, and thermodynamic parameters, *Amer. J. Nanom.*, 9 (2021) 1-11. <http://pubs.sciepub.com/ajnan/9/1/1>
- [26] J.A. Naser, T.A. Himdan, A.J. Ibraheim, Adsorption kinetic of malachite green dye from aqueous solutions by electrospun nanofiber Mat, *Orient. J. Chem.*, 33 (2017) 3121-3129. <http://dx.doi.org/10.13005/ojc/330654>
- [27] A.B. Fradj, A. Boubakri, A. Hafiane, S.B. Hamouda, Removal of azoic dyes from aqueous solutions by chitosan enhanced ultrafiltration, *Res. Chem.*, 2 (2020) 100017. <https://doi.org/10.1016/j.rechem.2019.100017>

- [28] C. Xia, Y. Jing, Y. Jia, D. Yue, J. Ma, X. Yin, Adsorption properties of congo red from aqueous solution on modified hectorite: Kinetic and thermodynamic studies, *Desalination*, 265 (2011) 81-87. <https://doi.org/10.1016/j.desal.2010.07.035>
- [29] B. Obradović, Guidelines for general adsorption kinetics modeling, *Hemi. Ind.*, 74 (2020) 65-70. <https://doi.org/10.2298/HEMIND200201006O>
- [30] Y. Kuang, X. Zhang, S. Zhou, Adsorption of methylene blue in water onto activated carbon by surfactant modification, *Water*, 12 (2020) 587. <https://doi.org/10.3390/w12020587>
- [31] S. Debnath, U.C. Ghosh, Kinetics, isotherm and thermodynamics for Cr(III) and Cr(VI) adsorption from aqueous solutions by crystalline hydrous titanium oxide, *J. Chem. Therm.*, 40 (2008) 67-77. <https://doi.org/10.1016/j.jct.2007.05.014>
- [32] A.S. Özcan, B. Erdem, A. Özcan, Adsorption of Acid Blue 193 from aqueous solutions onto Na-bentonite and DTMA-bentonite, *J. Coll. Inter. Sci.*, 280 (2004) 44-54. <https://doi.org/10.1016/j.jcis.2004.07.035>